

Microscopic characterization of the photocatalytic oxidation of oxalic acid adsorbed onto TiO₂ by FTIR-ATR

Cecilia B. Mendive^{a,b,c,*}, Detlef W. Bahnemann^a, Miguel A. Blesa^{b,c,1}

^a *Institut für Technische Chemie, Universität Hannover, Callinstr. 3, D-30167 Hannover, Germany*

^b *Unidad de Actividad Química, Centro Atómico Constituyentes, Comisión Nacional de Energía Atómica, Avenida General Paz 1499, 1650 San Martín, Provincia de Buenos Aires, Argentina*

^c *Consejo Nacional de Investigaciones Científicas y Técnicas, Avenida Rivadavia 1917, 1033 Capital Federal, Argentina*

Available online 19 March 2005

Abstract

Sequential FTIR-ATR spectra of an illuminated Degussa P-25 film deposited onto the ATR crystal were recorded to follow the photocatalytic oxidation of oxalic acid in acidic media. The results show that illumination ensues in the depletion of adsorbed oxalate from its equilibrium condition. The equilibrium spectral and thermodynamic data obtained previously from measurements in the dark were used to derive the time evolution, upon illumination, of the surface coverage of each of the three known surface complexes formed by oxalic acid adsorbed onto TiO₂. The results demonstrate that the most stable species is also the most photo-labile one, and that the surface speciation is determined by a fast surface redistribution among the three species, without equilibration with the bulk solution. Thus, zero-order kinetics are observed at high degrees of coverage during the disappearance of the least stable species. At low concentrations, the disappearance of the most stable species is characterised by first-order kinetics.

© 2005 Elsevier B.V. All rights reserved.

Keywords: Surface phenomena; TiO₂; Oxalic acid; Photocatalytic degradation

1. Introduction

Oxalic acid is a simple model compound of pollutants that contain more than one carboxylate group, and its behaviour during its heterogeneous photocatalytic oxidation should be representative for some of the main features of the whole class of organic acids. The interaction of oxalate with the photocatalyst surface in the dark has been thoroughly characterised by FTIR-ATR spectroscopy [1–4] and several papers have reported the kinetics of its photocatalytic degradation [5–10]. Oxalic acid is easily oxidised to carbon dioxide, thus minimising the problem of possible accumulation of intermediate products; its primary oxidation product, the radical anion CO₂^{•−} injects its electron into the

conduction band and produces a second CO₂ molecule. Only if the pH is adequately high, carbonate may be retained at the photocatalyst's surface.

In this work, we report the results of a FTIR study of the changes that occur upon illumination of the surface of a thin TiO₂ layer in the presence of aqueous oxalic acid. Sequential spectra were obtained during a series of experiments that span a wide range of oxalic acid concentrations and light intensities. In a previous publication [11], we had shown that this technique was useful to characterise the formation of intermediates as well as the depletion caused by the photocatalytic oxidation of adsorbed catechol. Catechol forms only one surface complex, and thus the interpretation of the spectral data under illumination is straightforward. Oxalic acid, on the other hand, is known to form three different surface complexes and because of this the interpretation of the results is complicated and requires thorough mathematical analysis. In this work, we show that the use of the attenuated total reflection fourier transform infrared spectroscopy (ATR-FTIR) [12,13] technique

* Corresponding author. Tel.: +49 511 762 5560.

E-mail addresses: hansmann@iftc.uni-hannover.de (C.B. Mendive), bahnemann@iftc.uni-hannover.de (D.W. Bahnemann), miblesa@cnea.gov.ar (M.A. Blesa).

¹ Tel.: 54 11 6772 7007.

permits to characterise the time evolution of each of these surface complexes during the photocatalytic oxalate degradation. Information about the surface reaction mechanism can thus be obtained directly and the understanding of the photocatalytic process can be improved.

2. Experimentals

2.1. Materials

Titanium dioxide used throughout this study was Degussa P-25, composed mainly of anatase, with a rutile content of around 15%. Primary particle size is ca. 30 nm and BET surface area of this non-porous material is $50 \text{ m}^2 \text{ g}^{-1}$. All other reagents were analytical grade and used as received. All solutions were prepared with MilliQ water from a SARTORIUS ARIUM 611 apparatus (conductance = $18.2 \text{ M}\Omega \text{ cm}^{-1}$).

2.2. Methods—the TiO_2 particles layer

A thin layer of immobilized TiO_2 particles was deposited on the surface of the ATR ZnSe crystal in the following way: a TiO_2 suspension was prepared at a concentration of 4.24 g L^{-1} and dispersed by sonication for 15 min in an ultrasonic cleaning bath. An aliquot of $300 \mu\text{L}$ of this suspension was placed on the surface of the crystal. With the tip of the pipette this small volume was spread in order to evenly cover the surface of the crystal. The thin layer of suspension was directly evaporated to dryness at room temperature with the help of a vacuum pump. To remove the excess of not-well adhering particles from the surface, a gentle stream of water was used followed by a drying process as described before. This final layer of particles thus obtained has a thickness of $1.7 \pm 0.3 \mu\text{m}$ (AFM measurements [1]), equivalent to a coverage of 2.3 g m^{-2} .

On the one hand, employing these conditions the evanescent wave of infrared light can probe the film properly to obtain the desired informations concerning the species formed at the surface of the particles [1–3]. On the other hand, they have been chosen to be able to use data from a previous work [2] carried out under exactly the same experimental conditions. These data correspond to the independent components of the experimental spectra, obtained by single value decomposition (SVD) together with global analysis [1–3] using the characteristic parameters of the material from Ref. [1].

The use of these layers, which remain stable over the entire course of the experiment, allows us to assume that the effective path lengths at all wavelengths remain unchanged. We also assume that the layer is isotropic, since the particles are small and randomly orientated, and uniformities in the layer thickness are averaged over the area of the ATR plate. Once the layer had been prepared, the coated crystal was mounted in the FTIR equipment.

2.3. Methods—adsorption and photocatalytic experiments

The TiO_2 -coated crystal was allowed to equilibrate with 3 mL oxalic acid-free aqueous solution for 32 min; during this period of time, sequential spectra were collected at intervals of 213.6 s (approximately 3.56 min). When the last spectrum had been recorded, the UV lamp was turned on and another sequence of spectra was recorded during 32 min at the same time intervals. These two groups of spectra were considered as the blank reference spectra in the dark and under illumination, respectively. The illuminated blank spectra were recorded in order to have a pre-illumination step before the TiO_2 particles were brought in contact with the oxalic acid solution. This procedure assures the removal of surface contaminants through photocatalytic destruction (e.g., oxidation) reactions and thus, avoids an induction-type behaviour characteristic for the oxidation of residual organic material originating from the catalyst preparation [14].

Immediately after the blank spectra were recorded, the solution on the TiO_2 layer was replaced by 3 mL oxalic acid solution and the spectra were collected in the same way, i.e., in the dark and under illumination.

The final spectra were obtained by subtracting the corresponding blank.

FTIR spectra of several aqueous oxalic acid solutions (ATR-FTIR) of increasing values of concentration were obtained to determine the upper limit at which the signal due to dissolved oxalic acid becomes negligible. This concentration was found to be a little higher than $2.00 \times 10^{-3} \text{ mol L}^{-1}$.

The oxalic acid solutions were prepared in 0.01 mol L^{-1} KCl at pH 3.60 (adjusted by adding KOH or HCl).

2.4. Methods—the equipment

FTIR spectra were recorded at 25°C , using a BOMEM MB 122 instrument equipped with a liquid N_2 cooled MCT-A detector. A horizontal Spectra Tech ZnSe-ATR unit 45° was used. The spectrometer was constantly purged with argon to avoid H_2O and CO_2 contamination. The final spectral resolution was 4 cm^{-1} since every scan is a double scan of two simple scans with a resolution of 8 cm^{-1} (from low frequencies to higher ones and in the opposite direction) interlaced by the equipment. Each final spectrum is the average of 250 scans. Base line corrections were made in order to eliminate minor fluctuations due to instrumental instabilities. The spectra were not smoothed and no ATR corrections were made.

The lamps used were two UV-A tubes (PHILIPS CLEO 15 W), which have a maximum of emission at wavelengths between 300 and 400 nm.

The energy outputs of the lamps were checked daily employing an UV-meter Dr. Hönle/UV-technology.

The semi-micro pH-electrode was a Mettler Toledo Inlab[®] 423 combined with a reference electrode Ag/AgCl.

3. Results

Fig. 1 shows the time evolution in the dark of the adsorbed oxalic acid spectra at pH 3.60 for total initial oxalic acid concentrations of $2.0 \times 10^{-3} \text{ mol L}^{-1}$ (A) and $6.5 \times 10^{-4} \text{ mol L}^{-1}$ (B), respectively. In both cases, the adsorption process is characterised by two stages. A first rapid step which corresponds to approximately 15% of the time required by the system to reach the equilibrium and takes place while the first spectrum is recorded (~ 4 min), followed by a slower process in which the absorption peak at 1726 cm^{-1} gains further intensity. This behaviour is observed at both oxalic acid concentrations studied. After 20–23 min, the equilibrium with the surface is reached.

The final equilibrated spectra have been shown previously [1,2] to correspond to the formation of three different complexes of the oxalic molecule on the TiO_2 surface, characterised by the structures and the Langmuir-type constants given in Table 1. The spectral changes observed during the slowest step of equilibration are associated with the build up of the least stable species, which has a characteristic band at 1726 cm^{-1} . Although it is possible to fit the data of the latter stage in Fig. 1 to a simple pseudo first-order kinetic equation, the experimental information is not sufficient to derive with any desirable precision the rate constant, which has been reported to be around $5 \times 10^{-3} \text{ s}^{-1}$ at a total oxalate concentration of $6.5 \times 10^{-4} \text{ mol L}^{-1}$. Previous work [2] also showed that in the dark, adsorption is essentially complete within 15 min.

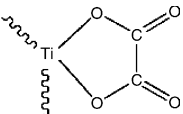
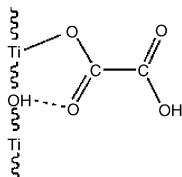
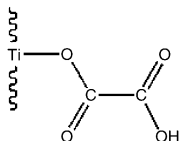
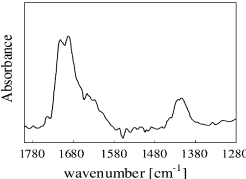
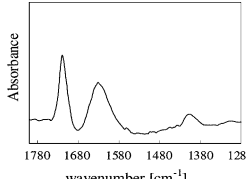
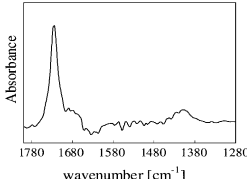
Desorption rates are appreciably slower. The replacement of salicylate for oxalate has been described previously [2]; its substitution takes place in a time span of 4 h when the incoming ligand concentration is $10^{-3} \text{ mol L}^{-1}$ at pH 3.7. As salicylate adsorption is considerably faster than that of oxalate [2], this time span corresponds to a rate control by the oxalate desorption.

Figs. 2 and 3 show the time evolution of the spectra during the illumination with UV-A light, for the two explored initial oxalic acid concentrations and total energy inputs of 1.0 and 0.6 mW cm^{-2} , respectively. Similar data, not shown, were obtained for other concentrations and at an irradiance of 0.6 mW cm^{-2} . An important decrease in absorbance occurs already during the time interval before the first spectrum is recorded (~ 4 min). The spectral changes in the following time intervals suggest a change in the surface speciation, compatible, at least qualitatively, with the expected changes in surface speciation due to a decrease in the total oxalate surface concentration and, in particular, with the disappearance of the least stable complex, i.e., the last complex formed during the dark adsorption.

However, the evolution of the spectra after light has been shut off, do not support this conclusion. Fig. 4 shows three spectra corresponding to: the last spectrum recorded in the dark (adsorption equilibrium) for a total initial oxalic acid concentration of $1.3 \times 10^{-3} \text{ mol L}^{-1}$, the last spectrum recorded under illumination (1.0 mW cm^{-2}) for the same system, and a third spectrum of the same system in the dark

Table 1

Langmuir stability constants (K_L), band assignments, structure and calculated spectra of the three surface complexes formed by the chemisorption of oxalate onto TiO_2 at 25°C and pH 3.60

Surface complexes			Assignment
I	II	III	
Maxima absorbance bands (cm^{-1})			
1712; 1692	1719	1726; ~ 1680 b	$\nu(\text{C=O})$
	1631		$\nu_a(\text{CO}_2^-)$
1415	1405	1409 b	$\nu(\text{C-O}) + \nu(\text{C-C})$
1310 w	1305 w	1308 vw	$\nu_s(\text{CO}_2^-)$
1268 w	1252 w	1254 w	$\nu(\text{C-O}) + \delta(\text{O-C=O})$
Proposed structure and their calculated spectra (SVD-global analysis)			
			
			
$\log(K_L/M)$ 6.38	4.48	3.48	

b: broad; w: weak; vw: very weak. The spectra and the values of the constants were obtained through SVD-Global Analysis (taken from Ref. [2]).

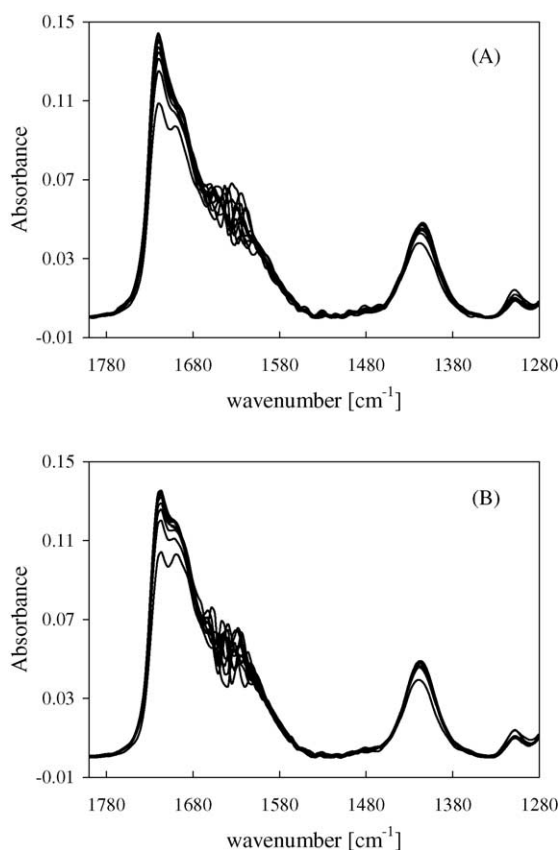


Fig. 1. Sequential FTIR-ATR spectra of oxalate adsorbed onto TiO_2 (Degussa P-25) in the dark at pH 3.60 and room temperature. The time axis must be read sequentially from bottom to top. The time intervals are of 213.6 s between every spectrum. Initial oxalate concentration: (A) $2.00 \times 10^{-3} \text{ mol L}^{-1}$; (B) $0.65 \times 10^{-3} \text{ mol L}^{-1}$.

again, recorded approximately 4 min after the illumination has been turned off. Comparison of the two latter spectra shows that the spectral features associated with the weakest complex regain part of their lost intensity in the dark. This result demonstrates that the total oxalate surface concentration has decreased during photolysis beyond the values expected from adsorption equilibrium considerations. Absorbance changes observed under UV-A illumination will thus be partially compensated by changes pointing towards the opposite direction, until the equilibrium with the residual bulk oxalic acid concentration is again attained.

Our experimental conditions precluded any measurement of the remnant aqueous oxalic acid concentration because of the small available volume of the aqueous phase and the poor response of the HPLC equipment for the quantification of very low concentrations of oxalic acid in aqueous solutions. Such measurements could be carried out when catechol was the photolyte [11]; in this system, the remnant concentration has also been shown to be higher than the equilibrium value (corresponding to the total measured surface concentration).

Concerning the pH of the system, it is not possible to control it while the experiment proceeds under our experimental conditions, but only one measurement was

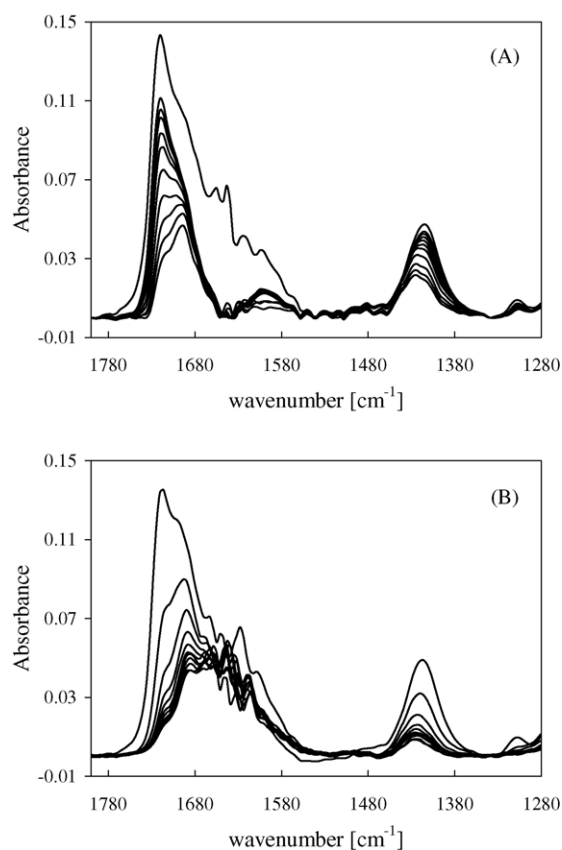


Fig. 2. Sequential FTIR-ATR spectra of oxalate adsorbed onto TiO_2 (Degussa P-25), observed after successive periods of illumination at a total energy input of 1.0 mW cm^{-2} , initial pH 3.60 and room temperature. The time axis must be read sequentially from top to bottom. The first spectrum corresponds to the equilibrium (in the dark), the following spectra correspond to the same system under illumination. The time intervals were of 213.6 s between every spectrum. Initial oxalate concentration: (A) $2.00 \times 10^{-3} \text{ mol L}^{-1}$; (B) $0.65 \times 10^{-3} \text{ mol L}^{-1}$.

possible at the end of each experiment (following the illumination period). These data show an increase in the pH value, as illustrated in Table 2. This effect is observed both in blank experiments, and in the presence of oxalic acid.

From the data in Table 2, part of the observed pH change must be attributed to the degradation (photodegradation) of

Table 2
Initial and final (after the illumination period) pH values observed during the experiments at the two different light intensities employed and for the two total initial oxalic acid concentrations

Light intensity (mW cm^{-2})	Sample (mol L^{-1})	pH _{initial}	pH _{final}
1.0	0.01 KCl (blank)	3.50	3.83
	2×10^{-3} oxalic acid	3.59	4.63
1.0	0.01 KCl (blank)	3.50	4.06
	6.5×10^{-4} oxalic acid	3.59	6.37
0.6	0.01 KCl (blank)	3.51	4.03
	2×10^{-3} oxalic acid	3.59	4.66
0.6	0.01 KCl (blank)	3.51	Not measured
	6.5×10^{-4} oxalic acid	3.59	6.36

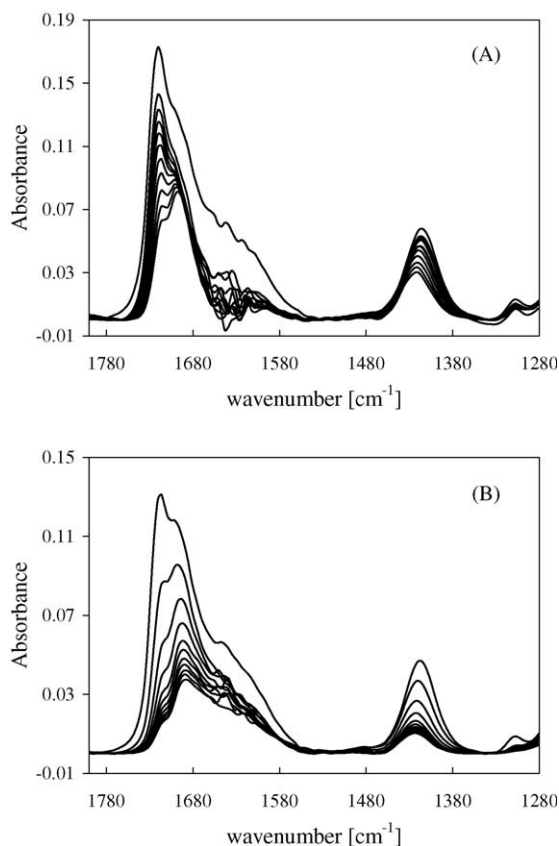


Fig. 3. Sequential FTIR-ATR spectra of oxalate adsorbed onto TiO₂ (Degussa P-25), observed after successive periods of illumination at a total energy input of 0.6 mW cm⁻², initial pH 3.60 and room temperature. The time axis must be read sequentially from top to bottom. The first spectrum corresponds to the equilibrium (in the dark), the following spectra correspond to the same system under illumination. The time intervals were of 213.6 s between every spectrum. Initial oxalate concentration: (A) 2.00 × 10⁻³ mol L⁻¹; (B) 0.65 × 10⁻³ mol L⁻¹.

the ATR crystal, as shown in Eq. (1). In addition, the reaction progress of the photocatalytic oxalate oxidation should also be accompanied by an irreversible pH increase; the stoichiometric proton consumption per mole of oxidised oxalate depends on the solution speciation of oxalate and on the fraction of total oxalate that is adsorbed. Assuming that dissolved oxalate is present mainly as the monoanion HC₂O₄⁻, and that adsorption may be described essentially as the dissociative chemisorption of H₂C₂O₄, the number of protons consumed for each mole of oxidised oxalate is expected to be between 1 (see Eq. (6)) and 0 (see Eq. (7)).

The formation of a precipitate on the ZnSe crystal that could only be removed by polishing the crystal with diamond paste, was noticed after long irradiation times. We believe that this attack of the ATR crystal is linked with the production of H₂Se (Eq. (1)) that decomposes partially to leave a residue of elemental Se, which a probable mechanism is illustrated with the sequence of Eqs. (1)–(5). In this case, the H₂Se formed due to the low pH leads to the formation of elemental Se and H₂. The holes and

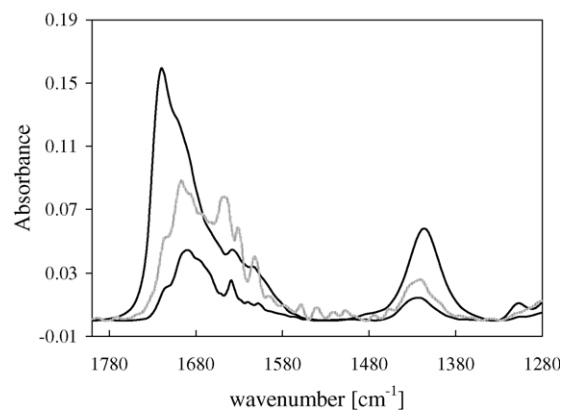


Fig. 4. In full lines, from top to bottom: the last spectrum recorded in the dark (adsorption equilibrium) for a total initial oxalic acid concentration of 1.3 × 10⁻³ mol L⁻¹ and the last spectrum recorded under illumination (after approximately 32 min at 1.0 mW cm⁻²) for the same system. In dashed lines: the spectrum of the same system in the dark again, approximately 4 min later after illumination has been turned off.

electrons photogenerated in the TiO₂ would oxidize anions Se²⁻ and reduce H⁺, respectively.

Because of the probable attack of the crystal and the eventual change in the experimental conditions due to the resulting pH change, the illumination time was kept to approximately half an hour as a compromise to collect enough information of the kinetic degradation process and to protect the integrity of the crystal.

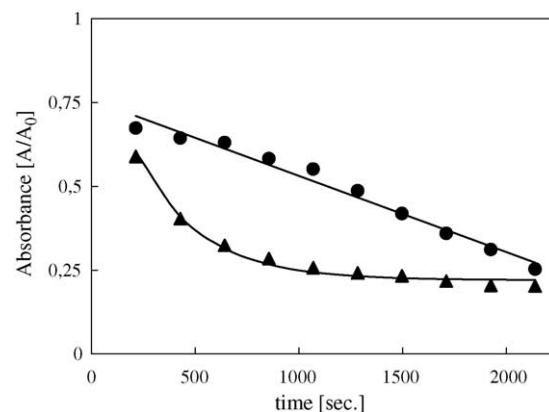
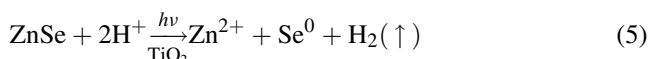
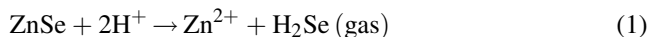


Fig. 5. Time evolution of the integrated area between 1793.6 and 1681.8 cm⁻¹. Total oxalic acid concentration: (●) 2.00 × 10⁻³ mol L⁻¹; (▲) 0.65 × 10⁻³ mol L⁻¹. Total energy input: 1.0 mW cm⁻².

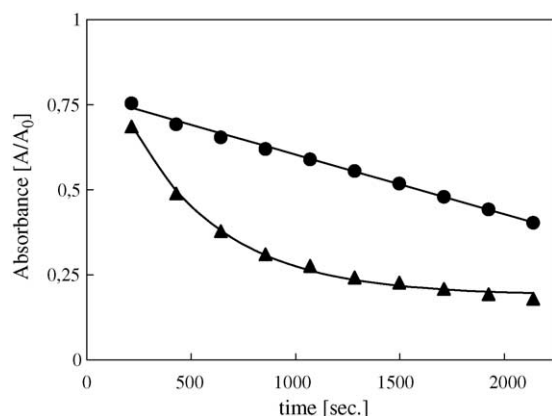


Fig. 6. Time evolution of the integrated area between 1793.6 and 1681.8 cm^{-1} . Total oxalic acid concentration: (●) $2.00 \times 10^{-3} \text{ mol L}^{-1}$; (▲) $0.65 \times 10^{-3} \text{ mol L}^{-1}$. Total energy input: 0.6 mW cm^{-2} .

Fig. 5 shows the time evolution of the relative spectral area (A/A_0) in the absorbance interval between 1793.6 and 1681.8 cm^{-1} under illumination, as derived from the data in Fig. 2. Fig. 6 shows analogous data for a lower light intensity, corresponding to an energy input of 0.6 mW cm^{-2} , as derived from the data in Fig. 3. At the highest surface coverage (highest total oxalic acid concentration), after a fast initial decrease (not shown), the area decreases linearly with time; at the lowest surface coverage, however, the band area decreases exponentially with time.

The comparison of the slopes of the linear absorbance decreases at the two light intensities (Figs. 5 and 6) evinces that the kinetic order on light intensity is 0.90, with $2.00 \times 10^{-3} \text{ mol L}^{-1}$ being the total initial oxalic acid concentration. For the first-order kinetic behaviour observed at the lower oxalate concentration (Figs. 5 and 6), the corresponding order on light intensity is 0.40, with $0.65 \times 10^{-3} \text{ mol L}^{-1}$ being the total initial oxalic acid concentration.

4. Discussion

Assuming that all spectra can be described as a linear combination of the spectra corresponding to the three surface complexes that have previously been identified for the adsorption of oxalic acid onto titania surfaces [1,2], the assessment of the contribution of each species to the total signal at each photolysis time was possible using the absorbance at three conveniently selected wavelengths. This procedure was found to yield better results, rather than using the whole spectral signal and process it by means of single value decomposition together with global analysis because of the lack of extensive spectral data at various oxalate concentrations.

Thus, the absorbance (A_λ) of a band centred at a given wavelength λ can be written as a function of the degree of coverage θ_i and the absorbance at total coverage, $A_{i\lambda}^0$, with

$i = 1-3$ for each of the three respective complexes (I–III) given in Table 1 (Eq. (8)).

$$A_\lambda = \theta_1 A_{1\lambda}^0 + \theta_2 A_{2\lambda}^0 + \theta_3 A_{3\lambda}^0 \quad (8)$$

The $A_{i\lambda}^0$ values for the three wavelengths were taken from the previous study of the equilibrated adsorption of oxalate in the dark [2], and the values of θ_i corresponding to the spectra recorded under light were calculated using three experimental A_λ values. In principle, such values could be totally arbitrarily chosen since every set of three absorbance wavelengths should lead to the same calculated θ_i , so we decided to choose those wavelengths near the maximum of each complex (1689.5, 1720.37 and 1724.23 cm^{-1} , respectively, for complexes I–III). It is also important to remark that other calculations were performed with different sets of chosen wavelengths to check the consistence of the calculations.

Although the absolute values thus derived (approximate θ_i) may be affected by the use of spectral information obtained under different conditions (from Ref. [2]), the dependence upon irradiation time should be independent of any systematic error of the procedure.

Figs. 7 and 8 show normalised plots of the resulting approximate θ_1 , θ_2 and θ_3 as a function of time as calculated

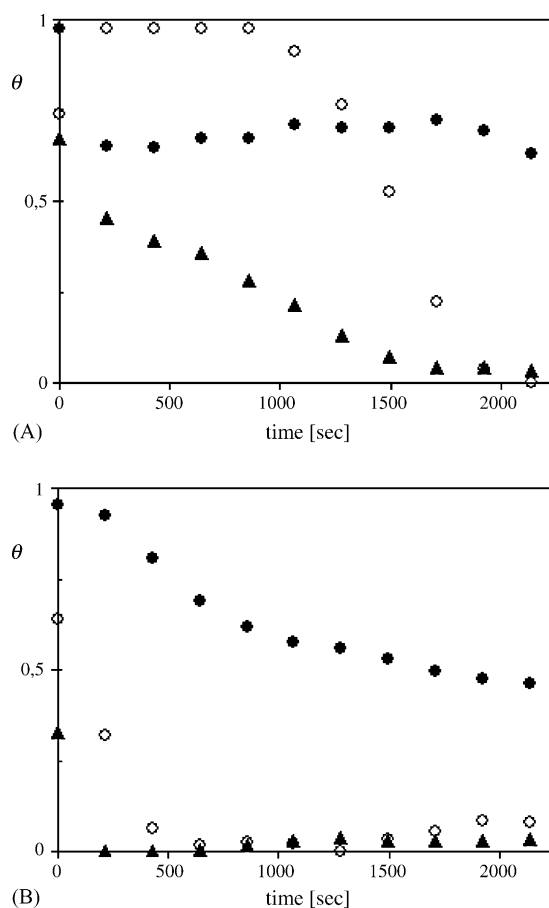


Fig. 7. Time evolution of the degrees of coverage θ_i for the three surface complexes. (●) θ_1 , (○) θ_2 and (▲) θ_3 . Total oxalic acid concentration: (A) $2.00 \times 10^{-3} \text{ mol L}^{-1}$; (B) $0.65 \times 10^{-3} \text{ mol L}^{-1}$. Total energy input: 1.0 mW cm^{-2} .

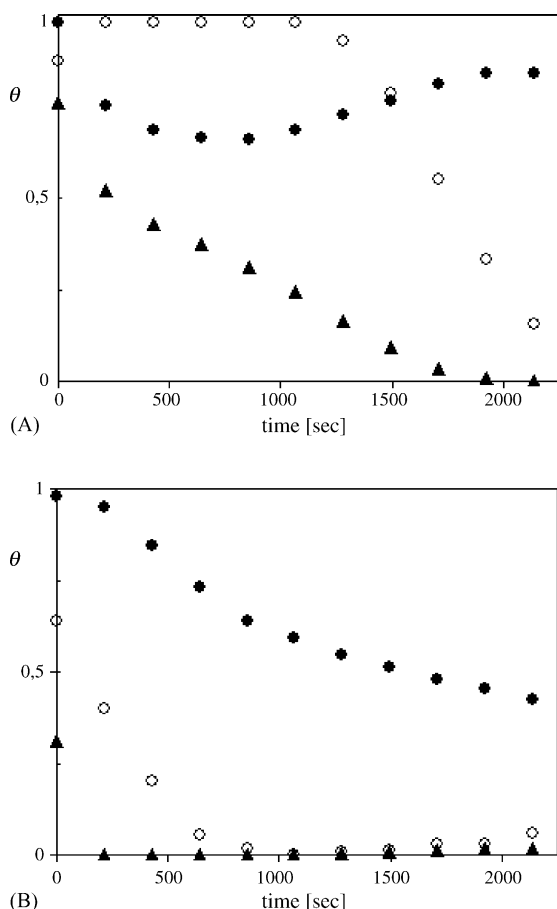


Fig. 8. Time evolution of the degrees of coverage θ_i for the three surface complexes. (●) θ_1 , (○) θ_2 and (▲) θ_3 . Total oxalic acid concentration: (A) $2.00 \times 10^{-3} \text{ mol L}^{-1}$; (B) $0.65 \times 10^{-3} \text{ mol L}^{-1}$. Total energy input: 0.6 mW cm^{-2} .

from the data shown in Figs. 2 and 3. Normalisation was done by setting the initial θ_i values equal to the corresponding dark equilibrium values.

If the effect of irradiation time was simply a decrease in the dissolved oxalate concentration, the ratio $\theta_1:\theta_2:\theta_3$ should evolve along the abscissa axis in a similar fashion as for a dark equilibrated surface when the total degree of coverage decreases. Assuming that the surface and the solution are equilibrated at all times, the ratio $\theta_1:\theta_2:\theta_3$ is given by Eq. (9), where K stands for the Langmuir constant, and $[\text{Ox}]$ is the concentration of dissolved oxalate (equilibrium concentration).

$$\theta_1 : \theta_2 : \theta_3 = \frac{K_1}{1 + K_1[\text{Ox}]} : \frac{K_2}{1 + K_2[\text{Ox}]} : \frac{K_3}{1 + K_3[\text{Ox}]} \quad (9)$$

Changes in pH can also produce changes in the equilibrium condition, through the pH dependence of the Langmuir constants, with changes in surface speciation. It has been pointed out earlier [3] that it is reasonable to assume that all forms of chemisorption involve the dissociative coordination of oxalic acid, with the same proton stoichiometry. Thus, changes in pH at a given oxalate concentration should produce changes in surface speciation similar to those produced by

changes in oxalate concentration at fixed pH; Hug and Sulzberger [1] do indeed report this behaviour. Thus, at least part of the trends observed in θ_i are due to the pH rise.

However, it has already been noted that the illuminated surface is partially depleted, to recover slowly in the dark after illumination is turned off (Fig. 4); the recovery of spectral intensity in the dark indicates that, further to changes due to the observed irreversible pH drift, light induces depletion from equilibrium surface conditions. The time span for recovery of the spectral intensity may be controlled by the rate of oxalate adsorption (cf. Fig. 1) or, more likely, by the slow release of adsorbed CO_2 protolysis species or mass transfer limitations.

Although the plots of θ_i as a function of time are rough approximations, the trends observed in Figs. 7 and 8 demonstrate that, as long as traces of the least stable complex are present, depletion is associated with its removal, whilst the surface concentration of the other species does not change much. Thus, speciation changes induced by illumination resemble the changes in equilibrium speciation produced by a decrease in the concentration of oxalate or an increase in pH. As the data in Fig. 4 rule out fast exchange of the ligand between the surface and the bulk solution, conducive to a surface that is equilibrated with the solution at all times, surface rearrangement seemingly takes place without mediation of the dissolved species. Within the surface, the equilibrium condition between the three species is given by the expressions (10) and (11).

$$\frac{\theta_1}{1 - \theta_1} : \frac{\theta_2}{1 - \theta_2} : \frac{\theta_3}{1 - \theta_3} = K_1 : K_2 : K_3 \quad (10)$$

$$\theta_1 + \theta_2 + \theta_3 = 3\theta_T \quad (11)$$

The time evolution of θ_1 , θ_2 and θ_3 provides evidence of fast surface rearrangements. Fast surface equilibration is also indicated by the observed changes in kinetic order at high and low θ_T . At high oxalate concentrations, $\theta_T \cong 1$; under these conditions, irrespective of which complex undergoes photolysis, θ_1 should remain close to 1, and should not change drastically with time, as observed. The zero-order kinetics (see Figs. 5 and 6) suggest that the most stable complex I is the one undergoing photocatalytic degradation initially, and that the evolution of the surface composition can be described by Fig. 9 and the scheme of reactions (12)

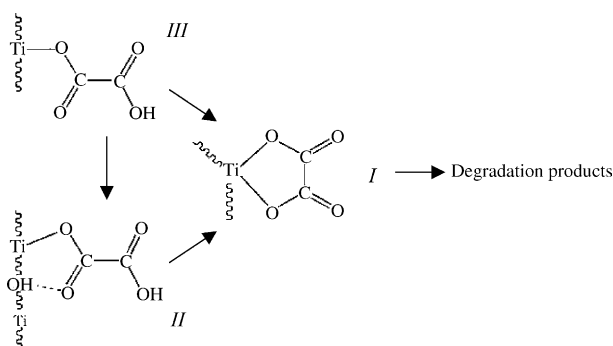
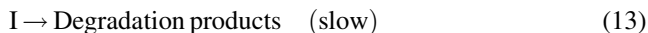
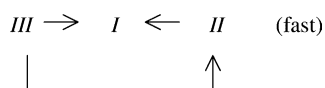


Fig. 9. Schematic evolution of the surface composition under illumination.

and (13) where I–III are the surface complexes given in Table 1.



In the dark, the half-life $t_{1/2}$ for the process of replenishment of complex III from the solution is short; i.e., the buildup of III has a $t_{1/2}$ of the order of 3 min. However, under illumination, the desorption of the degradation products (mainly HCO_3^-) or other ill-defined surface rearrangements may limit the rate. The rate of ligand exchange is known to be slower, as observed in mixtures of oxalate and salicylate [2].

At high degrees of coverage, the photocatalytic oxidation reaction is limited by the light availability; accordingly, the apparent order on light intensity is high, although less than unity. The non-compliance to an order of 1 must be attributed to an increase in recombination rates with increasing light intensity. On the other hand, at low total oxalate concentration, when $\theta_1 \cong \theta_T < 1$, the depletion of I produced by photolysis cannot be compensated by surface migration from other species, and the kinetics of degradation becomes first-order in I. The results shown in Figs. 5 and 6 support these conclusions. Comparison of these figures shows a kinetic order on light intensity for the case of high coverage of 0.40. This lower value suggests an increased recombination due to the scarcity of the hole traps.

The preferential photolysis of the most stable complex suggests that hole trapping by the surface complex may be involved, the most effective trap being the most stable complex because of the strong interaction of the negatively charged oxalate molecule with surface Ti(IV) resulting in the deepest, i.e., lowest lying, energy traps for holes. Although preferential attack by adjacent $\bullet\text{OH}$ radicals cannot be ruled out on the basis of our data alone, high selectivity as observed in this study in an $\bullet\text{OH}$ mediated mechanism does not seem plausible.

All these conclusions must be accepted with some caution, because of the variety of involved processes, and the limitations of the experimental evidence. In particular, the comparisons of the apparent rates at two different concentrations of oxalate is limited by the different pH shift attending the reactions in each case, and the ensuing different contribution from thermal desorption to the observed spectral changes, as discussed above. Ideally, an experimental set up permitting to fix the pH during photolysis should be used to eliminate ambiguities in the interpretation. These types of experiments are being carried on at present.

5. Conclusions

The photocatalytic oxidation of oxalate on the surface of TiO_2 proceeds through the most stable surface complex. During this process, the other species replenish the surface availability of this most stable complex. Under our experimental conditions, interchange between adsorbed and dissolved oxalate is slow as compared to photocatalytic destruction of the surface complexes, and a depletion of the total oxalate surface complexes is observed by illumination.

Acknowledgements

Work supported by European Union (Project INCO ICA4-2002-1000), as well as by research grants from Millennium Performance Chemicals Ltd., ANPCyT, CNEA and CONICET. MAB is a member of the Research Career of CONICET. CBM is a Fellowship holder of CONICET. We want to thank Mr. Christian Maassen for helpful technical support.

References

- [1] S.J. Hug, B. Sulzberger, *Langmuir* 10 (1994) 3587.
- [2] A.D. Weisz, L. García Rodenas, P.J. Morando, A.E. Regazzoni, M.A. Blesa, *Catal. Today* 76 (2002) 103.
- [3] A.D. Weisz, A.E. Regazzoni, M.A. Blesa, *Solid State Ionics* 143 (2001) 125.
- [4] C.B. Mendive, A.D. Weisz, M.A. Blesa, Presented at the 11th International Conference on Surface and Colloid Science, Iguazu Falls, Brazil, 15–19 September 2003.
- [5] Z.D. Draganic, I.G. Draganic, M.M. Kosanic, *J. Phys. Chem.* 68 (1964) 2085.
- [6] Z.D. Draganic, M.M. Kosanic, M.T. Nenadovic, *J. Phys. Chem.* 71 (1967) 2390.
- [7] J.-M. Herrmann, M.-N. Mozzanega, P. Pichat, *J. Photochem.* 22 (1983) 333.
- [8] M.M. Kosanic, *J. Photochem. Photobiol. A: Chem.* 119 (1998) 119.
- [9] K. Kobayakawa, C. Sato, Y. Sato, A. Fujishima, *J. Photochem. Photobiol. A: Chem.* 118 (1998) 65.
- [10] T.A. McMurray, J.A. Byrne, P.S.M. Dunlop, J.G.M. Winkelman, B.R. Eggins, E.T. McAdams, *Appl. Catal. A: Gen.* 262 (2004) 105.
- [11] P.Z. Araujo, C.B. Mendive, L.A. García Rodenas, P.J. Morando, A.E. Regazzoni, M.A. Blesa, D. Bahnemann, *Colloids Surf.*, in press.
- [12] S.T. Martin, J.M. Kesselman, D.S. Park, N.S. Lewis, M.R. Hoffmann, *Environ. Sci. Technol.* 30 (1996) 2535.
- [13] S.J. Hug, *J. Colloid Interface Sci.* 188 (1997) 415.
- [14] C. Wang, C. Böttcher, D.W. Bahnemann, J.K. Dohrmann, *J. Mater. Chem.* 13 (2003) 2322.